

Structural characterization and immunostimulatory activity of polysaccharides from *Brassica rapa* L.

Zhuo-Er CHEN, Reziyamu WUFUER, Jin-Hu JI, Jin-Fang LI, Yu-Feng CHENG, Caixia Dong, and Hailiqian TAOERDAHONG

J. Agric. Food Chem., **Just Accepted Manuscript** • DOI: 10.1021/acs.jafc.7b03902 • Publication Date (Web): 10 Oct 2017

Downloaded from <http://pubs.acs.org> on October 10, 2017

Just Accepted

“Just Accepted” manuscripts have been peer-reviewed and accepted for publication. They are posted online prior to technical editing, formatting for publication and author proofing. The American Chemical Society provides “Just Accepted” as a free service to the research community to expedite the dissemination of scientific material as soon as possible after acceptance. “Just Accepted” manuscripts appear in full in PDF format accompanied by an HTML abstract. “Just Accepted” manuscripts have been fully peer reviewed, but should not be considered the official version of record. They are accessible to all readers and citable by the Digital Object Identifier (DOI®). “Just Accepted” is an optional service offered to authors. Therefore, the “Just Accepted” Web site may not include all articles that will be published in the journal. After a manuscript is technically edited and formatted, it will be removed from the “Just Accepted” Web site and published as an ASAP article. Note that technical editing may introduce minor changes to the manuscript text and/or graphics which could affect content, and all legal disclaimers and ethical guidelines that apply to the journal pertain. ACS cannot be held responsible for errors or consequences arising from the use of information contained in these “Just Accepted” manuscripts.

Structural characterization and immunostimulatory activity of polysaccharides from *Brassica rapa* L.

Zhuo-Er CHEN¹ ^{||}, Reziyamu WUFUER¹ ^{||}, Jin-Hu JI², Jin-Fang LI³, Yu-Feng CHENG¹,
Cai-Xia DONG^{4*}, Hailiqian TAOERDAHONG^{1*}

¹College of Pharmacy, Xinjiang Medical University, Urumqi, Xinjiang Uygur Autonomous Region, China;

²Medical Engineering Technology Institute, Xinjiang Medical University, Urumqi, Xinjiang Uygur Autonomous Region, China;

³The Experimental Teach Center, College of HouBo, Xinjiang Medical University, Karamay, Xinjiang Uygur Autonomous Region, China;

⁴Tianjin Key Laboratory on Technologies Enabling Development of Clinical Therapeutics and Diagnosis, School of Pharmacy, Tianjin Medical University, Tianjin 300070, China.

Corresponding Authors

*(C.-X.D.) Tel: +86-183-2247-3708; E-mail: dongcaixia@tmu.edu.cn

*(H.T.) Tel: +86-139-9987-9870; E-mail: hailiqian2471@sina.com

Author Contributions

^{||}Z.-R.C. and R.W. contributed equally.

ABSTRACT

1 Two neutral polysaccharides (BRNP-1 6.9 kD, BRNP-2 4.8 kD) were purified from
2 the common edible plant *Brassica rapa* L. via the combined techniques of ion-exchange
3 chromatography and high-performance gel permeation chromatography. Monosaccharide
4 composition analysis showed that BRNP-1 and BRNP-2 were composed of glucosyl
5 residues. Methylation and 1D- and 2D-NMR analyses revealed that both BRNP-1 and
6 BRNP-2 contained a backbone chain that was composed of α -D-(1 \rightarrow 4)-linked Glcp
7 residues and side chains that were composed of terminally linked Glcp residues attached at
8 the O-6 position of backbone-glycosyl residues. BRNP-1 and BRNP-2, however, differed
9 in branch degree and molecular weight. Bioassay results showed that treatment with the
10 higher dosage (400 μ g/mL) of BRNP-1 and BRNP-2 stimulated the proliferation, NO
11 release, and cytokine secretion (IL-6 and TNF- α) of RAW264.7 macrophages. These
12 results suggested that BRNP-1 and BRNP-2 may enhance macrophage-mediated immune
13 responses.

14 **KEYWORDS:** *Brassica rapa* L., polysaccharides, structural characterization,
15 immunostimulatory activity

1. INTRODUCTION

16 The innate immune system comprises macrophages, monocytes, granulocytes, and
17 humoral elements¹. Macrophages, the first line of immune defense, perform a variety of
18 complex biological activities, including phagocytosis, surveillance, chemotaxis, and
19 destruction of targeted organisms². These activities suggest that regulating macrophage
20 activity is a potential strategy against disease³. In recent years, many kinds of plant-derived
21 polysaccharides have been widely investigated by researchers because of their
22 immunostimulatory activity on macrophages⁴, such as water-soluble polysaccharide (SNP)
23 from *Sipunculus nudus* L.⁵, a *Laminaria japonica* polysaccharide⁶, and Ginseng fruits
24 polysaccharides⁷, as well as Astragalus polysaccharides⁸⁻¹⁰, and polysaccharides from
25 *Tinospora cordifolia*¹¹. And studies demonstrated that polysaccharides may mainly exert
26 immunomodulatory effects on macrophage RAW264.7 via TLR4-mediated
27 MyD88-dependent signaling pathways⁸⁻¹¹.

28 *Brassica rapa* L., a common edible plant that belongs to the family of Cruciferae, is
29 widely distributed at high-altitude regions in Xinjiang Uyghur Autonomous Region, China.
30 The root of *B. rapa* is a traditional Uyghur folk medicine for moistening lungs and
31 relieving cough and asthma¹². Studies have shown that the pharmacological activities of *B.*
32 *rapa* result from its nutritional benefits, including vitamins¹³, glucosinolates¹⁴, flavonoids¹⁵,
33 ferredoxin-sulfite reductase¹⁶, chalcone glycosides¹⁷, and polysaccharides^{18,19}. Among
34 them, glucosinolates (GLSs) have attracted the more attention in view of their
35 chemopreventive activities against numerous chronic degenerative diseases, together with
36 cancer, cardiovascular diseases, neurodegeneration and diabetes.^{14,18} Compared with GLSs,
37 however, polysaccharides as the main water-soluble components in *B. rapa* were few
38 investigated, especially in structural characterization^{18,19}. It has been reported that only
39 three polysaccharides with relatively low molecular weight¹⁸ and three polysaccharides

40 with large molecular weight¹⁹ were isolated from *B. rapa*. However, there is no more
41 information reported on the structural characterization except the monosaccharide
42 composition. In addition, increasing evidence over recent years has demonstrated that
43 polysaccharides exhibit immunomodulatory activity. Experimental evidence for the
44 immunomodulatory activities of other plant-derived polysaccharides and the use of *B. rapa* as
45 traditional folk medicine imply that polysaccharides from *B. rapa* may also have
46 immunomodulatory activity. To the best of our knowledge, however, no other studies have
47 investigated polysaccharides from *B. rapa* and their immunological activity. In this paper,
48 we report the isolation, structural characterization, and in *vitro* immunostimulatory
49 activity of polysaccharides from *B. rapa* L.

2. MATERIALS AND METHODS

50 **2.1 Materials.** *B. rapa* roots were collected from a commercial market in Urumqi,
51 Xinjiang Uygur, Autonomous Region of China. Toyopearl DEAE 650 M was purchased
52 from Tosoh (Tokyo, Japan). PL aquagel-OH MIXED-H (7.5 mm × 300 mm, 8 μm) and
53 Sugar-pack TM (6.5 mm × 300 mm, 10 μm) columns were purchased from Agilent (USA)
54 and Waters Co., respectively. Sepharose 6B and Sephacryl S-300 HR were obtained from
55 GE Healthcare (Amersham Biosciences AB, Uppsala, Sweden). Other chemicals were
56 obtained from Sigma-Aldrich Co. LLC. Fetal bovine serum (FBS), trypsin, Dulbecco
57 Modified Eagle Medium (DMEM), phosphate buffered solution (PBS), streptomycin,
58 penicillin, and dimethyl sulfoxide (DMSO) were obtained from Hyclone Co. (UT, USA).
59 Lipopolysaccharide (LPS) was purchased from Sigma Chemical Co. (MO, USA). Cell
60 Counting Kit-8 (CCK-8 kit), and IL-6 and TNF-α ELISA kits were purchased from Wuhan
61 Boster Co. (Wuhan, China). Nitric oxide (NO) kit was supplied by Promega Co.
62 (Wisconsin, USA).

63 HPLC analyses were conducted on an Agilent 1200 system that was coupled with a

64 refractive index detector (RID). GC–MS analysis was performed on an Agilent GC-MS
65 7890A-5975 instrument with helium as the carrier gas. Fourier transform infrared (FT–IR)
66 spectra were recorded on a Nicolet 380 FT–IR spectrophotometer.

67 **2.2 Extraction, Isolation, and Purification of Polysaccharides.** Extraction was
68 performed in accordance with a previously described method²⁰. Dried *B. rapa* powder was
69 defatted by soaking in 95% ethanol (EtOH) at room temperature. After removing the
70 solvent, residues were extracted with hot water thrice for 2 h per extraction. The residues
71 were then filtered through defatted cotton and concentrated in vacuo. The supernatant was
72 precipitated with 80% EtOH. The precipitates were redissolved and dialyzed against
73 distilled water (cut off, 7000 Da). Crude *B. rapa* polysaccharides (BRP) were obtained
74 after freeze-drying.

75 BRP (3.0 g) was suspended in H₂O. The suspension was stirred at room temperature
76 and then centrifuged at 4000 rpm for 15 min to remove insoluble portions (17.6%). The
77 supernatant was then subjected to an ion-exchange chromatography on a Toyopearl DEAE
78 650 M column (5.0 i.d. × 20 cm). The supernatant was successively eluted with distilled
79 0.8 L of H₂O, 0.5 M, 1.0 M NaCl, 2.0 M NaCl, and 0.2 M NaOH to yield BRN (*B. rapa* L.
80 neutral polysaccharide fraction) (11.2%), BRA1 (32.9%), BRA2(0.7%), BRA3 (0.1%),
81 and BRA4 (1.4%), respectively. Fractions of 15 mL were collected and monitored at 490
82 nm via phenol–H₂SO₄ method²¹.

83 The water-eluted polysaccharide fraction BRN (500 mg) was loaded on a Sepharose
84 6B (5.0 i.d. × 90 cm) column and eluted with 0.1 M NaCl (1.2 L) to yield two major
85 fractions, BRN-1 and BRN-2. BRN-1 was further purified by gel filtration on Sephacryl
86 S-300 (2.2 i.d. × 90 cm) and eluted with 0.1 M NaCl (0.4 L) to yield BRNP-1 (240 mg).
87 BRN-2 was purified to yield BRNP-2 (250 mg). Fractions of 10 mL were collected and
88 monitored at 490 nm via phenol–H₂SO₄ method and at 280 nm via UV absorbance

89 spectroscopy.

90 **2.3 Estimation of Homogeneity and Apparent Molecular Weight.** The apparent
91 molecular weights of BRNP-1 and BRNP-2 were estimated with high-performance gel
92 permeation chromatography (HPGPC) analysis on an Agilent 1200 system equipped with
93 an RID detector. Samples (5 mg/mL, 10 μ L) were applied to a PL Aquagel-OH MIXED-H
94 column (7.5 mm \times 300 mm, 8 μ m) and eluted with 0.1M NaNO₃ at 0.6 mL/min with the
95 column temperature maintained at 35 °C. Commercially available T-series dextrans (MW
96 2000, 670, 410, 270, 150, 80, 50, 12, 5, and 1 kD) were used as standard molecular
97 markers.

98 **2.4 Colorimetric Analyses.** Total carbohydrate and uronic acid contents were
99 determined by phenol–sulfuric acid²¹ and m-hydroxybiphenyl²² methods with galactose as
100 the standard. Protein content was analyzed using a Bio-Rad protein assay kit with bovine
101 serum albumin (BSA) as the standard.

102 **2.5 Sugar Composition Analysis.** The sugar components of BRNP-1 and BRNP-2
103 were directly hydrolyzed with 2 M trifluoroacetic acid (TFA) at 120 °C for 2 h in
104 accordance with the routine method of complete hydrolysis for neutral polysaccharides.
105 After the removal of TFA under nitrogen gas, the hydrolysates were converted into alditol
106 acetates for GC–MS analysis, which was conducted with a fused silica capillary column
107 (HP-5 MS, 30 m \times 0.25 mm, 0.25 μ m, Agilent, USA). Injection and detector temperatures
108 were maintained at 280 °C. The oven temperature was programmed to increase from 160
109 °C to 190 °C at 2 °C/min, then to 240 °C at 5 °C/min, and maintained at 240 °C for 5 min.
110 Helium was used as the carrier gas.

111 **2.6 Methylation Analysis.** The methylation analyses of BRNP-1 and BRNP-2 were
112 performed in accordance with a previously described method²³. After posttreatment, the
113 resultant products were hydrolyzed with 2 M TFA at 120 °C for 2 h, followed by

114 reduction with NaBD₄ and acetylation with acetic anhydride to yield partially methylated
115 alditol acetates. These acetates were analyzed with GC–MS using a HP-5 MS fused silica
116 capillary column (30 m × 0.25 mm, 0.25 μm, Agilent). The column temperature was set to
117 120 °C during injection, then increased by 4 °C/min to 280 °C, and maintained at 280 °C
118 for 5 min. Helium was used as the carrier gas. Mass spectra were interpreted to identify
119 the compounds that corresponded to each peak. The molar ratio of each residue was
120 calculated on the basis of peak areas.

121 **2.7 Infrared Spectral Analysis.** The infrared spectra of the polysaccharide samples
122 were obtained with a FT–IR spectrophotometer. The purified polysaccharides were ground
123 with KBr powder and then pressed into a polymer film for FT–IR measurement in the
124 frequency range of 4000–400 cm⁻¹.

125 **2.8 NMR Analysis.** Approximately 20 mg BRNP-1 and BRNP-2 were dissolved in
126 0.6 mL D₂O and then analyzed via NMR at 30 °C. The maps of 1D- and 2D-NMR were
127 then obtained.

128 **2.9 Cell Line and Culture Medium.** The macrophage RAW 264.7 cell line was
129 purchased from the Cell Bank of Shanghai Institutes for Biological Sciences, Chinese
130 Academy of Sciences, Shanghai. The cell line was grown in DMEM medium that
131 contained 10% FBS and 100 U/mL of penicillin and 100 μg/mL of streptomycin.

132 **2.10 Macrophage Viability Test by CCK-8 Assay.** RAW 264.7 cells were seeded at
133 a density of 1.0×10^4 cells/mL in 96-well plates and cultured for 24 h at 37 °C in a
134 humidified incubator with 5% CO₂. Polysaccharide samples were added at the final
135 concentrations of 0, 1.6, 3.2, 8, 40, 80, 200, 400, 1000, and 2000 μg/mL. After 24 h of
136 incubation at 37 °C in 5% CO₂ humidified atmosphere, 10 μL of CCK-8 solution was
137 added to each well. After 1 h of incubation, absorbance was recorded at 450 nm using an
138 ELISA plate reader and then converted into macrophage viability ratio for comparison.

139 **2.11 Nitric Oxide Production and Cytokine Production after BRNP-1 and**
140 **BRNP-2 Treatment.** After 24 h of incubation in the above conditions, RAW 264.7 cells
141 (2×10^4 cells/mL) were treated with BRNP-1 and BRNP-2 (0, 80, or 400 $\mu\text{g/mL}$) or LPS (1
142 $\mu\text{g/mL}$) in DMEM medium. The treated cells were then incubated for an additional 24 h.
143 The conditioned culture medium was collected to analyze nitric oxide (NO) and cytokine
144 release by RAW 264.7 cells. NO, TNF- α , and IL-6 contents were determined using
145 commercial kits in accordance with the manufacturer's instructions. Cells that were treated
146 with 1 $\mu\text{g/mL}$ LPS were used as the positive control. Cells that were cultured in DMEM
147 medium without polysaccharides and LPS were used as the normal control.

148 **2.12 Statistical Analysis.** All experiments were repeated thrice. Results were
149 expressed as the mean \pm SD of triplicate analyses. Statistical significance was analyzed by
150 one-way ANOVA using SPSS 16.0 software. Comparisons with *P* values less than 0.05
151 were considered as statistically significant.

3. RESULTS AND DISCUSSION

152 **3.1 Structural Characterization of BRNP-1 and BRNP-2.** The purified
153 polysaccharides BRNP-1 and BRNP-2 were colorless, highly water-soluble powders. The
154 two polysaccharides were eluted as a single and symmetrical sharp peak on the HPGPC
155 chromatogram. As shown in Fig.1, these results indicated that BRNP-1 and BRNP-2 were
156 homogeneous. The apparent molecular weight of these polysaccharides were estimated as
157 6.9 kD and 4.8 kD from a dextran standard curve. The total carbohydrate, uronic acid, and
158 protein contents of BRNP-1 and BRNP-2 were determined through colorimetric analysis.
159 Results showed that carbohydrates dominated the chemical composition of BRNP-1
160 (99.8%) and BRNP-2 (99.9%), whereas protein was present only in trace amounts
161 (BRNP-1: 0.11%; BRNP: 0.07%). Uronic acid was not detected, thus suggesting that the
162 two polysaccharides are neutral polysaccharides.

163 The monosaccharide compositions of BRNP-1 and BRNP-2 were hydrolyzed and
164 acetylated intoalditol acetates for GC–MC analysis. As shown in Fig.2, only one peak
165 appeared at 21.1 min. Comparing the retention time of this peak with those of
166 authenticated standards revealed its identity as glucose (Glc). Therefore, BRNP-1 and
167 BRNP-2are composed of glucosyl residues.

168 The FT–IR spectra of BRNP-1 and BRNP-2 were similar (Fig. 3). The absorbance
169 band at 3409.3 cm^{-1} represented the stretching vibration of O–H bonds in constituent
170 sugar residues. Bands at approximately 2929.4 cm^{-1} were associated with the stretching
171 vibration of C–H in sugar rings. The band at approximately 1649.1 cm^{-1} indicated bound
172 water²⁴. Absorbance bands at 1154.1 cm^{-1} , 1078.0 cm^{-1} , and 1025.7 cm^{-1} indicated the
173 bending vibrational modes of C–O stretching in pyranose²⁵. In addition, the absorption
174 peak at 842.2 cm^{-1} suggestedthat glucosyl residues are mainly present in α -configuration²⁶,
175 whereas that at approximately 928.4 cm^{-1} isa characteristic of α -glucans²⁷. These wave
176 numbers indicated that the major glucosyl residues in these two polysaccharides are of
177 α -configuration and are α -glucans.

178 To identify the linkage type between glucosyl residues, BRNP-1 and BRNP-2 were
179 subjected to methylation analyses. Results are shown in Fig. 4 and are summarized in
180 Table 1.The total ionization chromatogram (TIC) showed that derivatized BRNP-1 and
181 BRNP-2 exhibited the same peak-signal pattern, which was composed of three peak
182 signals (1–3). These signals were identified based on the combination of fragment analysis
183 and monosaccharide composition results. Peak 1 was identified
184 as1,5-*di-O*-acetyl-(1-deuterio)-2,3,4,6-*tetra-O*-methyl glucitol as deduced from the major
185 primary ion fragments at m/z 161 and 162 that appeared in nearly equal amounts and the
186 diagnostic ion fragments at m/z 205 and 118.These ion fragments confirmed the presence
187 of *t*-linked Glcp²⁸. Peak 2 corresponded to the signal of

188 1,4,5-*tri-O*-acetyl-(1-deuterio)-2,3,6-*tri-O*-methyl glucitol, as deduced from the major
189 primary ion fragments at m/z 233 and 118 and the diagnostic fragment at m/z 162. These
190 fragments indicated the presence of (1→4)-linked Glcp units. As deduced from the
191 diagnostic pair m/z 118 and 261, peak 3 was assigned to
192 1,4,5,6-*tetra-O*-acetyl-(1-deuterio)-2,3-*di-O*-methyl glucitol, suggesting the presence of
193 (1→4,6)-linked Glcp²⁸. Taken together, both BRNP-1 and BRNP-2 were predominantly
194 composed of (1→4)-linked Glcp residues, suggesting the presence of a (1→4)-linked
195 glucan backbone. In addition, (1→4,6)- and *t*-linked Glcp residues were also present in
196 small amounts, indicating that the glucan backbone, which is attached by *t*-linked Glcp
197 residues, branches at the *O*-6 position. As summarized in Table 1, BRNP-1 and BRNP-2
198 exhibited similar glycosyl linkage composition but different apparent molecular weight
199 and branch degree (DB). DB was calculated according to the formula²⁹(DB) =
200 (NT+NB)/(NT+NB+NL), where NT, NB, and NL are the total numbers of the terminally
201 linked residues, branched residues, and linear residues, respectively. On the basis of this
202 formula, the DB values of BRNP-1 and BRNP-2 were calculated as 0.243 and 0.238,
203 respectively.

204 To further interpret the structures of BRNP-1 and BRNP-2, the two polysaccharides
205 were analyzed via 1D- (¹H- and ¹³C-NMR) and 2D-NMR (HSQC and HMBC). The
206 obtained spectra were data from the literature. As shown in Fig.5A-a, the ¹H-
207 and ¹³C-NMR spectra of these two polysaccharides have similar signal patterns. In the
208 low-field region, three anomeric hydrogen signals appeared at δ 4.5-5.5 ppm in ¹H-NMR
209 spectra. These signals corresponded to three anomeric carbon signals at δ 90–110 ppm in
210 ¹³C-NMR spectra. Taking the results of methylation analysis into consideration, the
211 presence of these anomeric signals suggested three glucopyranosyl residues in the
212 repeating units of BRNP-1 and BRNP-2. In the case of BRNP-1, signals at δ 4.88 (98.63),

213 5.30 (99.83), and 5.27 (100.02) ppm were assigned to the H1 (C1) of *t*-linked Glcp residue
214 (residue A), (1→4)-linked Glcp residue (residue B), and (1→4, 6)-linked Glcp residue
215 (residue C), respectively. Consistent with the results of IR analysis, the signals in the
216 lower field indicated that all glucosyl residues have α -configuration. In high field, the
217 major signals at δ 3.76, 3.87, 3.57, 3.55, and 3.77/3.76 in ^1H -NMR spectrum were
218 assigned to H-2, H-3, H-4, H-5, and H-6a/H-6b of residue B in accordance with the
219 literature^{30,31}. Corresponding carbons were easily determined from correlations in HSQC,
220 as summarized in Table 2. Other signals were assigned by the combination of 2D-NMR
221 and evidence from the literature^{30,31}.

222 The linkage sequence was deduced from HMBC spectra (Fig.5B-b). A strong
223 cross-peak signal at δ 3.57/99.83 ppm was assigned to the correlation between H-4 and
224 C-1 of inter-residue B, suggesting a (1→4)- α -linked glucan backbone. This deduction was
225 also supported by the weak cross-peak signal at δ 5.30/77.12 ppm; on the basis of data
226 from the literature, this signal was ascribed to the correlation between the H-1 and C-4 of
227 inter-residue B³⁰. In addition, a very weak cross-peak signal at 4.88/69.44 ppm was
228 attributed to the correlation between the H-1 (δ 4.88) of residue A and the C-6 (δ 69.44) of
229 residue C, indicating that the H-1 of residue A is linked to the O-6 of residue C. In
230 accordance with the results of methylation analysis, deductions from the HMBC spectra
231 suggested that BRNP-1 contains a (1→4)-linked glucan backbone that branches at the O-6
232 position by *t*-linked Glcp residues.

233 BRNP-2 showed similar ^1H - and ^{13}C -NMR and HMBC spectra (not shown here) as
234 BRNP-1, suggesting that BRNP-1 and BRNP-2 have similar structural characteristics.
235 Considering all of the information obtained from NMR spectra and methylation analyses,
236 both BRNP-1 and BRNP-2 contain a (1→4)- α -linked glucan backbone chain that branches
237 at the O-6 position of the backbone units with *t*- α -linked Glcp residues as side chains. The

238 two polysaccharides, however, differ in apparent molecular weight and DB. The possible
239 structures of BRNP-1 and BRNP-2 are shown in Fig. 6.

240 **3.2 Immunomodulatory Activity of BRNP-1 and BRNP-2.** The cytotoxicity of
241 BRNP-1 and BRNP-2 against RAW 264.7 macrophages was evaluated by CCK-8 assay.
242 The viability of control wells (no sample) was considered to be 100%. The viability ratios
243 of macrophages that were activated by samples were determined at the indicated
244 concentrations. As shown in Fig.7A, BRNP-1 showed low cytotoxicity at the low
245 concentration of 1.6–80 $\mu\text{g/mL}$, exerted no cytotoxicity at concentrations higher than 80
246 $\mu\text{g/mL}$, and exhibited the best stimulatory activity on macrophages at 400 $\mu\text{g/mL}$.
247 BRNP-2 exhibited significant proliferation activity in a dose-dependent manner and
248 exerted no cytotoxic effects at concentrations of 1.6 to 2000 $\mu\text{g/mL}$. Thus, our results
249 revealed that higher concentrations of BRNP-1 and BRNP-2 stimulate macrophage
250 proliferation. Therefore, the concentrations of 80, 400 $\mu\text{g/mL}$ of BRNP-1 and BRNP-2
251 were used as treatments in the following experiments.

252 NO is released from various mammalian cells, including vascular endothelial cells,
253 macrophages, mesangial cells, spleen lymphocytes, glial cells, and fibroblasts. As a
254 messenger molecule, NO exerts cytotoxic effects on bacteria, fungi, and tumor cells, and
255 is implicated in inflammatory responses in response to tissue injury³². We determined NO
256 production from RAW 264.7 cells treated with BRNP-1 and BRNP-2 to evaluate their
257 activation effects on macrophages. As shown in Fig. 7B, treatment with higher dosage
258 (400 $\mu\text{g/mL}$) of BRNP-1 or BRNP-2 on RAW264.7 cells significantly enhanced the
259 release of NO in the culture medium compared with that in the normal control group,
260 especially for BRNP-1 which showed even a comparative level compared to LPS group.
261 As compared with the normal control group, however, treatment with the lower dosage (80
262 $\mu\text{g/mL}$) of BRNP-1 or BRNP-2 showed no significant effect on the release of NO. It is

263 well known that NO is a major mediator of macrophages and essential for the resistance of
264 immune system to pathogens invasion. Glucans that are composed of 1,4- α -D-glucosidic
265 linkages have been reported to have a significant effect on NO production from
266 macrophages³³. In our study, both BRNP-1 and BRNP-2 stimulated the NO release of
267 RAW 264.7 cells at higher dosage (400 μ g/mL). BRNP-1 showed more significant effects
268 on NO production than BRNP-2. Given the similar backbones and side chains of the two
269 polysaccharides, the different effects of BRNP-1 and BRNP-2 on NO production may be
270 closely related to molecular weight and DB.

271 We examined the ability of BRNP-1 and BRNP-2 to stimulate cytokine secretion in
272 macrophages. As illustrated in Fig. 7C, BRNP-1 or BRNP-2 exhibited a marked
273 enhancement in TNF- α secretion when treated RAW 264.7 cells at higher dosage 400
274 μ g/mL compared with the control group. The TNF- α secretion was observed to increase to
275 4.5 folds of that in control group with a level of 81 pg/mL, and 6.1 folds with a level of
276 110 pg/mL. BRNP-2 showed a stronger effect on TNF- α secretion than BRNP-1 at the
277 higher dosage. Consistent with the effect of two polysaccharides on the NO release, the
278 lower dosage of BRNP-1 and BRNP-2 showed little even suppressed effect on the TNF- α
279 secretion. Unlike the case in TNF- α , both BRNP-1 and BRNP-2 exhibited a significant
280 effect on the secretion of IL-6 (Fig. 7D) compared with that both in control group and in
281 LPS group, but no difference were observed between the higher and lower dosage
282 treatments.

283 The activation of macrophages results in the production of a large amount of NO. NO
284 contributes to the killing of pathogens and mediates a variety of biological functions as an
285 intracellular messenger molecule³⁴. In addition, macrophage activation produces various
286 cytokines, including TNF- α and IL-6. In turn, TNF- α and IL-6 induce the proliferation of
287 other immune cells, including B-cells and T-cells³⁵. In the present study, we found that

288 polysaccharides from *B. rapa* L. induced the activation of macrophages *in vitro*, as
289 manifested by NO production and cytokine (TNF- α and IL-6) secretion. Therefore, these
290 two polysaccharides may potentially enhance macrophage-mediated innate immune
291 response.

292 In summary, two neutral polysaccharides, BRNP-1 and BRNP-2, with apparent
293 molecular weights of 6.9 kD and 4.8 kD, respectively, were isolated from the medicinal
294 plant *B. rapa* L. via the combination of ion-exchange chromatography and
295 high-performance gel permeation chromatography. The structures of BRNP-1 and
296 BRNP-2 were characterized by chemical derivatization, HPGPC, GC-MS, and 1D- and
297 2D-NMR technologies. BRNP-1 contains a glucan backbone chain that is composed of
298 α -D-(1 \rightarrow 4)-linked Glcp residues. Moreover, BRNP-1 contains side chains that are
299 composed of *ft*-linked- α -D-Glcp residues that are attached at the O-6 position of
300 α -D-(1 \rightarrow 4)-linked Glcp at every eight backbone-glycosyl residues. Furthermore, the DB
301 of BRNP-1 is 0.243. BRNP-2 has the same backbone chain and side chains as BRNP-1
302 but differs in DB (0.238), which indicates that its side chains are attached at the O-6
303 position of α -D-(1 \rightarrow 4)-linked Glcp at every nine backbone-glycosyl residues. Bioassay
304 results showed that both BRNP-1 and BRNP-2 stimulate macrophage proliferation and
305 significantly enhance NO production and cytokine (TNF- α and IL-6) secretion when
306 treated RAW 264.7 cells with higher dosage of 400 μ g/mL. Therefore, BRNP-1 and
307 BRNP-2 may potentially enhance macrophage-mediated immune response. This study
308 provides preliminary information for further investigations on the antitumor effects of *B.*
309 *rapa* polysaccharides.

310

FUNDINGS

311 This work was financially supported by the National Natural Science Foundation of China

312 (No. 81460615), the Foundation of Key Laboratory of Xinjiang Uygur Autonomous
313 Region of China (XJDX0208-2012-1), and Tianjin Municipal Science and Technology
314 Commission (No. 15JCYBJC50700).

315

REFERENCES

- 316 (1) Chávez-Sánchez, L.; Espinosa-Luna, J. E.; Chávez-Rueda, K.; Legorreta-Haquet, M.
317 V.; Montoya-Díaz, E.; Blanco-Favela, F., Innate Immune System Cells in
318 Atherosclerosis. *Arch. Med.Res.* **2014**, *45*, 1-14.
- 319 (2) Sica, A.; Allavena, P.; Mantovani, A., Cancer related inflammation: the macrophage
320 connection. *Cancer Lett.* **2008**, *267*, 204-215.
- 321 (3) Grivennikov, S. I.; Greten, F. R.; Karin, M., Immunity, inflammation, and cancer. *Cell*.
322 **2010**, *140*, 883-899.
- 323 (4) Schepetkin, I. A.; Quinn, M. T., Botanical polysaccharides: macrophage
324 immunomodulation and therapeutic potential. *Int. Immunopharmacol.* **2006**, *6*,
325 317-333.
- 326 (5) Zhang, C. X.; Dai, Z. R., Immunomodulatory activities on macrophage of a
327 polysaccharide from *Sipunculus nudus* L. *Food Chem. Toxicol.* **2011**, *49*, 2961-2967.
- 328 (6) Zha, X.-Q.; Lu, C.-Q.; Cui, S.-H.; Pan, L.-H.; Zhang, H.-L.; Wang, J.-H.; Luo, J.-P.,
329 Structural identification and immunostimulating activity of a *Laminaria japonica*
330 polysaccharide. *Int. J. Biol. Macromol.* **2015**, *78*, 429-438.
- 331 (7) Wang, Y.; Huang, M.; Sun, R.; Pan, L., Extraction, characterization of a Ginseng fruits
332 polysaccharide and its immune modulating activities in rats with Lewis lung
333 carcinoma. *Carbohydr. Polym.* **2015**, *127*, 215-221.
- 334 (8) Wei, W.; Xiao, H.; Bao, W.; Ma, D.; Leung, C.; Han, X.; Ko, C.; Lau, C.; Wong, C.;
335 Fung, K.; Leung, P.; Bian, Z.; Han, Q. TLR-4 may mediate signaling pathways of

- 336 *Astragalus* polysaccharide RAP induced cytokine expression of RAW264.7 cells.*J.*
337 *Ethnopharmacol.* **2016**, *179*, 243-252.
- 338 (9) Zhou, L.; Wang, Z.; Yu, S.; Long, T.; Zhou, X.; Bao, Y., Astragalus polysaccharides
339 exerts immunomodulatory effects via TLR4-mediated MyD88-dependent signaling
340 pathway in vitro and in vivo., *Sci. Rep.* **2017**, *7*, 1-13.
- 341 (10)Zhang, W.; Ma, W.; Zhang, J.; Song, X.; Sun, W.; Fan, Y., The immunoregulatory
342 activities of Astragalus polysaccharide liposome on macrophages and dendritic cells.
343 *Int. J. Biol. Macromol.*, *2017*, in press.
- 344 (11)Kumar, G.P.; Rajan, M.G.R.; Kulkarni, S. Activation of murine macrophages by
345 G1-4A, a polysaccharide from *Tinospora cordifolia*, in TLR4/MyD88 dependent
346 manner. *Int. Immunopharmacol.* **2017**, *50*, 168-177.
- 347 (12)Liu, Y.M. *Brassica rapa* L. In *Uygur medicine tzu*, edition 1.; Liu, Y.M., Eds.; Health
348 science and technology publishing house in Xinjiang, China; 1999; Vol. 9.; pp.
349 334-335.
- 350 (13)Dominguez-Perles, R.; Mena, P.; Garcia-Viguera, C.; Moreno, D. A., Brassica foods
351 as a dietary source of vitamin C: a review. *Crit Rev Food Sci Nutr.* **2014**, *54*,
352 1076-1091.
- 353 (14)Jeong, J.; Park, H.; Hyun, H.; Kim, J.; Kim, H.; Oh, H. I.; Hwang, H. S.; Kim, D. K.;
354 Kim, H. H., Effects of glucosinolates from Turnip (*Brassica rapa* L.) root on bone
355 formation by human osteoblast-like MG-63 cells and in normal young rats. *Phytother*
356 *Res.* **2015**, *29*, 902-909.
- 357 (15)Annalisa R., P. V., Laura I., Francesca I., Daniela H., HPLC-DAD/MS
358 characterization of flavonoids and hydroxycinnamic derivatives in Turnip Tops
359 (*Brassica rapa* L. Subsp. *sylvestris* L.). *J.Agric. Food Chem.* **2006**, *54*, 1342-1346.
- 360 (16)Takahashi, S.; Yip, W. C.; Tamura, G., Purification and characterization of

- 361 ferredoxin-sulfite reductase from turnip (*Brassica rapa*) leaves and comparison of
362 properties with ferredoxin-sulfite reductase from turnip roots. *Biosci. Biotechnol.*
363 *Biochem.* **1997**, *61*, 1486-1490.
- 364 (17)Hara, H.; Nakamura, Y.; Ninomiya, M.; Mochizuki, R.; Kamiya, T.; Aizenman, E.;
365 Koketsu, M.; Adachi, T., Inhibitory effects of chalcone glycosides isolated from
366 *Brassica rapa* L. 'hidabeni' and their synthetic derivatives on LPS-induced NO
367 production in microglia. *Bioorg. Med. Chem.* **2011**, *19*, 5559-5568.
- 368 (18)Xie, Y.; Jiang, S.; Su, D.; Pi, N.; Ma, C.; Gao, P., Composition analysis and
369 anti-hypoxia activity of polysaccharide from *Brassica rapa* L. *Int. J. Biol. Macromol.*
370 **2010**, *47*, 528-533.
- 371 (19)Wang, W.; Wang, X.; Ye, H.; Hu, B.; Zhou, L.; Jabbar, S.; Zeng, X.; Shen, W.,
372 Optimization of extraction, characterization and antioxidant activity of
373 polysaccharides from *Brassica rapa* L. *Int. J. Biol. Macromol.* **2016**, *82*, 979-988.
- 374 (20)Bao-lin HOU, Q. W., HailiqianTaoerdahong., Research on polysaccharide extraction
375 and the content of *Brassica rapa*L. *Lishizhen Medicine And Materia Medica Research*
376 **2009**, *20*, 2759-2761.
- 377 (21)Dubois, M.; Gilles, K.A.; Hamilton, J.K.; Rebers, P.A.; Smith, F., Colorimetric
378 method for determination of sugars and related substances. *Anal. Chem.*, **1956**, *28*,
379 350-356.
- 380 (22)Blumenkrantz, N.; Asboe-Hansen, G., New method for quantitative determination of
381 uronic acids. *Anal. Biochem.* **1973**, *54*, 484-489.
- 382 (23)Ciucanu, I.; Kerek, F., A simple and rapid method for the permethylation of
383 carbohydrates. *Carbohydr. Res.* **1984**, *131*, 209-217.
- 384 (24) Parker, F.S., Application of I.R Spectroscopy in Biochemistry, In *Biology and*
385 *Medicine*, edition 1.; Parker, F.S., Eds.; Plenum Press, New York, 1971, Vol. 14.;

386 pp.100-104.

387 (25) Xu, F.; Liao, K.; Wu, Y.; Pan, Q.; Wu, L.; Jiao, H.; Guo, D.; Li, B.; Liu, B.,
388 Optimization, characterization, sulfation and antitumor activity of neutral
389 polysaccharides from the fruit of *Borojoa sorbilis* cuter. *Carbohydr. Polym.* **2016**, *151*,
390 364-372.

391 (26) Wu, Y.; Li, Y.; Liu, C.; Li, E.; Gao, Z.; Liu, C.; Gu, W.; Huang, Y.; Liu, J.; Wang, D.;
392 Hu, Y., Structural characterization of an acidic Epimedium polysaccharide and its
393 immune-enhancement activity. *Carbohydr. Polym.* **2016**, *138*, 134-142.

394 (27) Wang, Y.-Y.; Khoo, K.-H.; Chen, S.-T.; Lin, C.-C.; Wong, C.-H.; Lin, C.-H., Studies
395 on the immuno-modulating and antitumor activities of *Ganoderma lucidum* (Reishi)
396 polysaccharides: Functional and proteomic analyses of a fucose-containing
397 glycoprotein fraction responsible for the activities. *Bioorg. Med. Chem.* **2002**, *10*,
398 1057-1062.

399 (28) Carpita, N.C., Shea, E.M. Linkage structure of carbohydrates by gas
400 chromatography-mass spectroscopy (GC-MS) of partially methylated alditol acetates.
401 In *Analysis of Carbohydrate by GLC and MS*, edition 1.; Biermann, C. J., McGinnis,
402 G. D., Eds.; CRC Press, FL: Boca Raton, 1988; Vol. pp. 157-216.

403 (29) Tao, Y.; Zhang, L.; Fan, Y.; Wu, X., Chain conformation of water-insoluble
404 hyperbranched polysaccharide from fungus. *Biomacromolecules.* **2007**, *8*, 2321-2328.

405 (30) Xu, X.; Gu, Z.; Liu, S.; Gao, N.; He, X.; Xin, X., Purification and characterization of
406 a glucan from *Bacillus Calmette Guerin* and the antitumor activity of its sulfated
407 derivative. *Carbohydr. Polym.* **2015**, *128*, 138-146.

408 (31) Jiang, J.; Kong, F.; Li, N.; Zhang, D.; Yan, C.; Lv, H., Purification, structural
409 characterization and in vitro antioxidant activity of a novel polysaccharide from
410 *Boshuzhi*. *Carbohydr. Polym.* **2016**, *147*, 365-371.

- 411 (32)Huang, M.; Mei, X.; Zhang,S., Mechanism of nitric oxide production in macrophages
412 treated with medicinal mushroom extracts (Review). *Int.J.Med.Mushrooms*. **2011**, *13*,
413 1-6.
- 414 (33)Wu, D.-T.; Xie, J.; Wang, L.-Y.; Ju, Y.-J.; Lv, G.-P.; Leong, F.; Zhao, J.; Li, S.-P.,
415 Characterization of bioactive polysaccharides from *Cordyceps militaris* produced in
416 China using saccharide mapping. *J.Funct. Foods*. **2014**, *9*, 315-323.
- 417 (34)Baugh, J. A.; Bucala, R., Mechanisms for modulating TNF alpha in immune and
418 inflammatory disease. *Curr. Opin. Drug Disc*. **2001**, *4*, 635-650.
- 419 (35)Sobota, R. M.; Müller, P. J.; Khouri, C.; Ullrich, A.; Poli, V.; Noguchi, T.; Heinrich, P.
420 C.; Schaper, F., SHPS-1/SIRP1 α contributes to interleukin-6 signalling. *Cell. Signal*.
421 **2008**, *20*, 1385-1391.

422

423

424

425

426

427

428

429

430

431

432

433

434

435

Figure captions

436 **Fig. 1.** HPGPC chromatogram of polysaccharides BRNP-1 (A) and BRNP-2 (B). Samples
437 were applied to PL Aquagel-OH MIXED-H column (7.5mm×300mm, 8μm) and eluted
438 with 0.1M NaNO₃ at 0.6mL/min with column temperature maintained at 35 °C.
439 Commercially available T-series dextrans were used as standard molecular markers.

440 **Fig. 2.** GC-MS chromatograms of standard monosaccharides (A) and hydrolysates of
441 BRNP-1 (B) and BRNP-2 (C). Rha: rhamnose; Fuc: fucose; Ara: arabinose; Xyl: xylose;
442 Man: mannose; Glc: glucose; Gal: galactose.

443 **Fig. 3.** FT-IR spectrum of BRNP-1 and BRNP-2 between 400 and 4000cm⁻¹.

444 **Fig. 4.** GC-MS profile of partially methylated alditol acetates of BRNP-1. (A) TIC profile;
445 (B) MS fragments; (C) deduced residues. Peaks: 1, 1,5-*di-O*-acetyl-(1-deuterio)-2,3,4,6-
446 *tetra-O*-methyl glucitol; 2, 1,3,4-*tri-O*-acetyl-(1-deuterio)-2,3,6-*tri-O*-methyl glucitol; 3,
447 1,4,5,6-*tetra-O*-acetyl-(1-deuterio)-2,3-*di-O*-methyl glucitol.

448 **Fig. 5.** ¹³C and ¹H NMR spectra of BRNP-1 (A-a) and BRNP-2 (A-b) in D₂O as recorded
449 on a Varian INOVA 600 NMR spectrometer at 30 °C. HSQC (B-a) and HMBC (B-b)
450 spectra of BRNP-1 in D₂O as recorded on a Varian INOVA 600 NMR spectrometer at 30
451 °C.

452 **Fig. 6.** Predicted structure of the repeating units of BRNP-1 (A) and BRNP-2 (B).

453 **Fig.7.** The effect of BRNP-1 and BRNP-2 on the proliferation (A), NO production (B),
454 and TNF-α (C) and IL-6 (D) secretion of RAW264.7 macrophages. **P* < 0.05, vs the
455 control group; #*P* < 0.05, vs the LPS positive control group.

456

457

458

Table 1. The Deduced Glycosidic Linkage Type And Composition Of BRNP-1 And BRNP-2 Determined By Methylation And GC-MS Analyses

Sugar derivatives	mol%		Deduced residues
	BRNP-1	BRNP-2	
1,5- <i>di-O</i> -acetyl-(1-deuterio)-2,3,4,6- <i>tetr</i> <i>a-O</i> -methyl glucitol	14.9	15.3	t-Glcp
1,4,5- <i>tri-O</i> -acetyl-(1-deuterio)-2,3,6- <i>tri</i> - <i>O</i> -methyl glucitol	75.7	76.2	(1→4)-Glcp
1,4,5,6- <i>tetra-O</i> -acetyl-(1-deuterio)- -2,3- <i>di-O</i> -methyl glucitol	9.4	8.5	(1→4,6)-Glcp

Table 2. The ^1H -, ^{13}C -NMR Chemical Shifts of BRNP-1 Isolated From *Brassica rapa* L.

Glycosyl residues		Chemical shifts, δ (ppm)					
		1	2	3	4	5	6
<i>t</i> -Glc _p	H	4.97	3.51	3.95	3.68	3.87	3.68
	C	98.49	74.58	76.71	70.30	76.44	60.47
(1→4)-Glc _p	H	5.27	3.53	3.88	3.88	3.76	3.76
	C	99.67	71.42	73.27	76.54	71.18	60.43
(1→4,6)-Glc _p	H	5.30	3.50	3.55	3.57	3.88	3.33
	C	99.99	71.52	73.45	77.05	71.20	69.28

Fig. 1

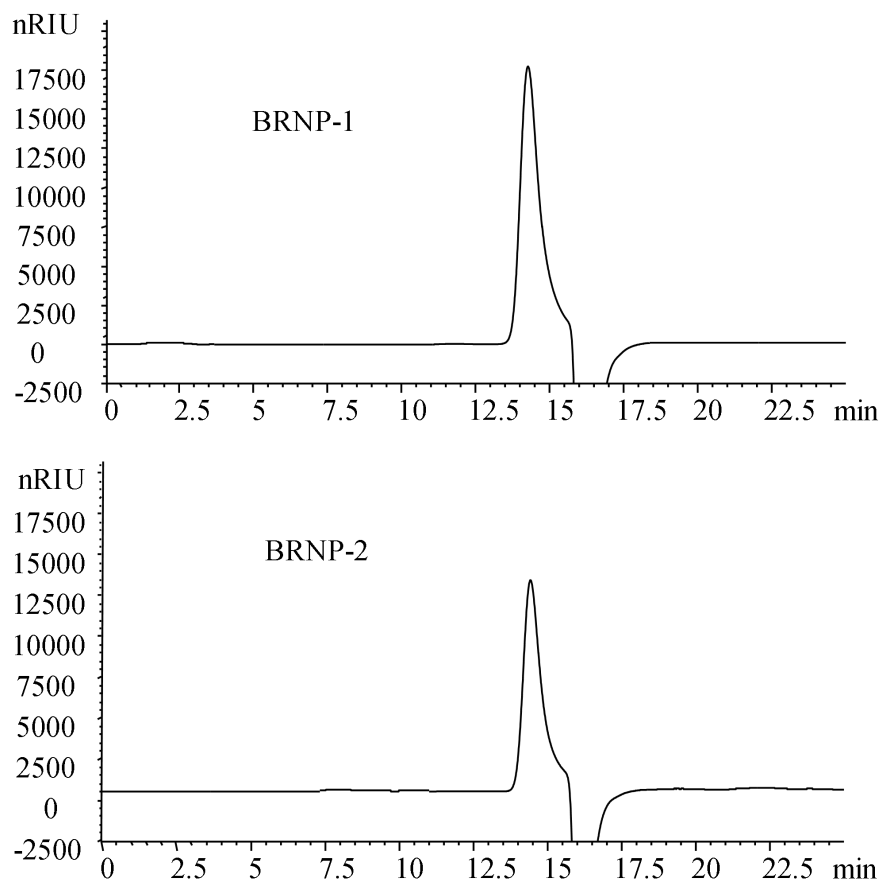


Fig. 2

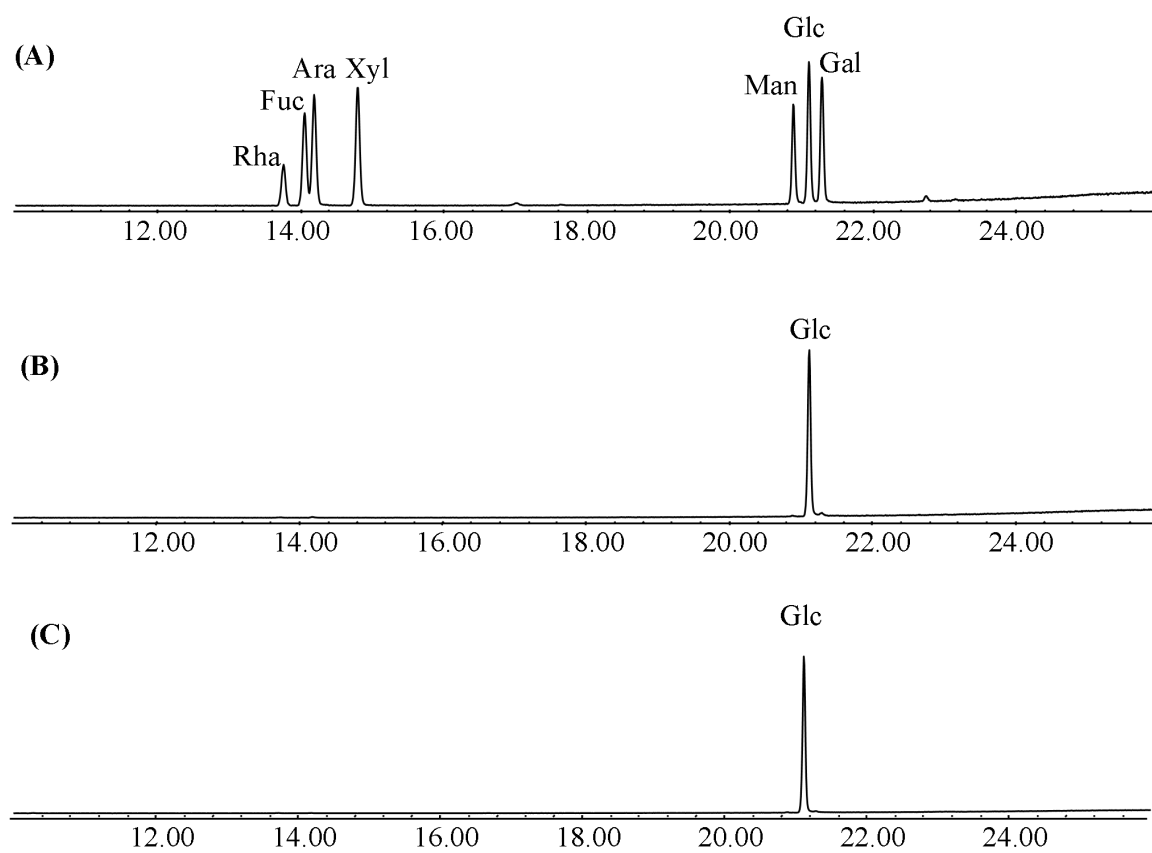


Fig. 3

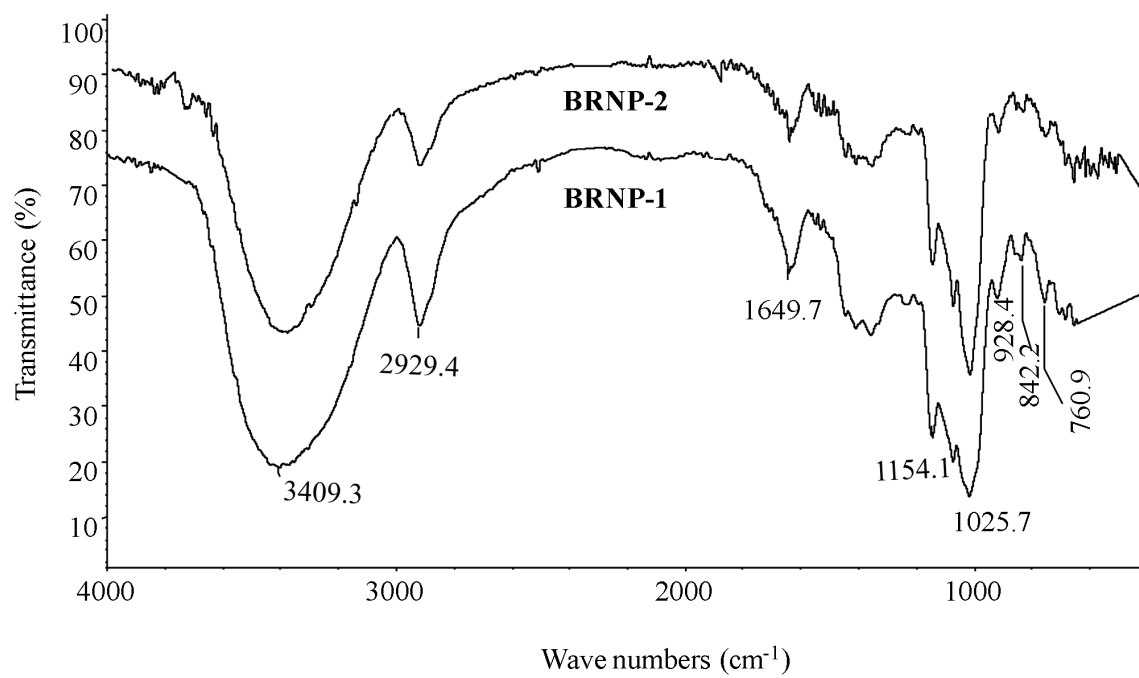


Fig. 4

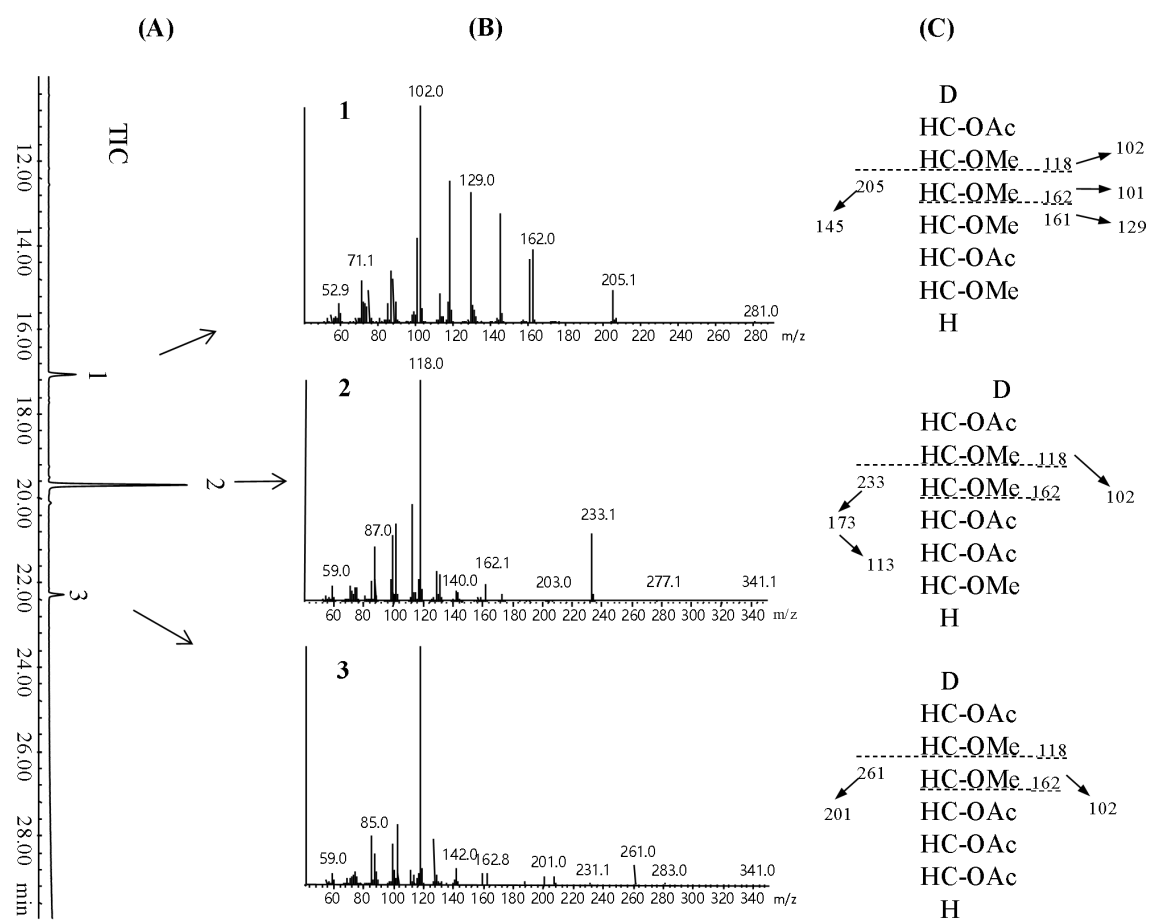


Fig. 5

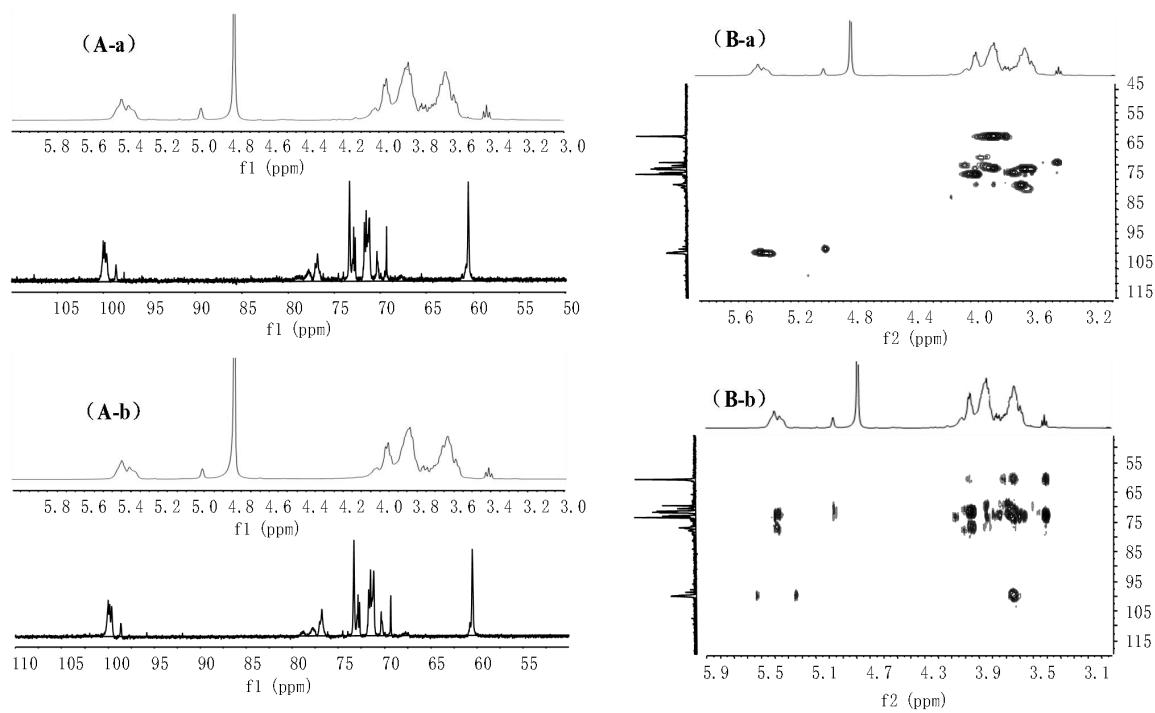


Fig. 6

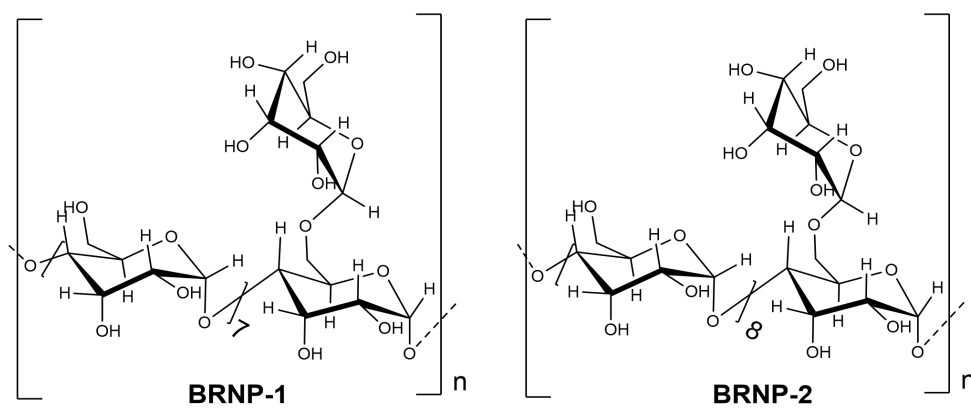
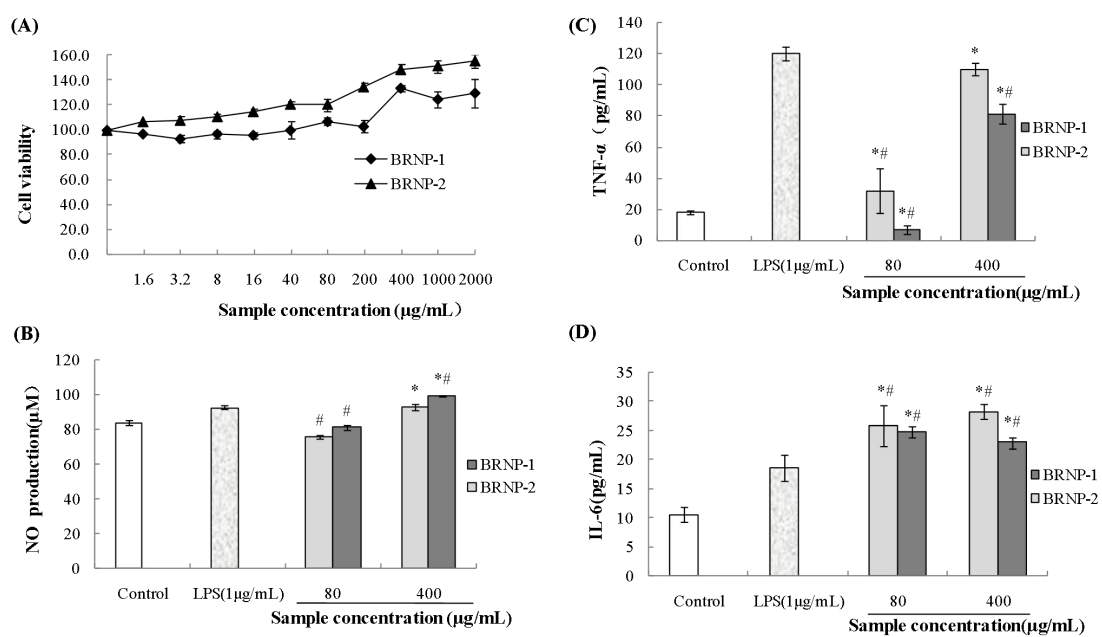


Fig. 7



TOC Graphic

